Dear Author,

Please, note that changes made to the HTML content will be added to the article before publication, but are not reflected in this PDF.

Note also that this file should not be used for submitting corrections.

AUTHOR QUERY FORM

ELSEVIER	**Journal: MEE** **Article Number: 9908**	**Please e-mail your responses and any corrections to:** **E-mail: corrections.esch@elsevier.sps.co.in**

Dear Author,

Please check your proof carefully and mark all corrections at the appropriate place in the proof (e.g., by using on-screen annotation in the PDF file) or compile them in a separate list. Note: if you opt to annotate the file with software other than Adobe Reader then please also highlight the appropriate place in the PDF file. To ensure fast publication of your paper please return your corrections within 48 hours.

For correction or revision of any artwork, please consult http://www.elsevier.com/artworkinstructions.

Any queries or remarks that have arisen during the processing of your manuscript are listed below and highlighted by flags in the proof. Click on the 'Q' link to go to the location in the proof.

Location in article	Query / Remark: click on the Q link to go Please insert your reply or correction at the corresponding line in the proof
Q1	Your article is registered as a regular item and is being processed for inclusion in a regular issue of the journal. If this is NOT correct and your article belongs to a Special Issue/Collection please contact p.das@elsevier.com immediately prior to returning your corrections.
Q2	Please confirm that given name(s) and surname(s) have been identified correctly.
Q3	Please check the telephone number of the corresponding author, and correct if necessary.
Q4	Highlights should only consist of 85 characters per bullet point, including spaces. The highlights provided are too long; please edit them to meet the requirement.
Q5	Please provide the year for Refs. [5,6,17,25–27].

Please check this box if you have no corrections to make to the PDF file ☐

Thank you for your assistance.

Graphical abstract

EWOD using nonaqueous liquids **pp xxx–xxx**

Maziar Ahmadi, Sandra Bermejo *, Luis Castañer

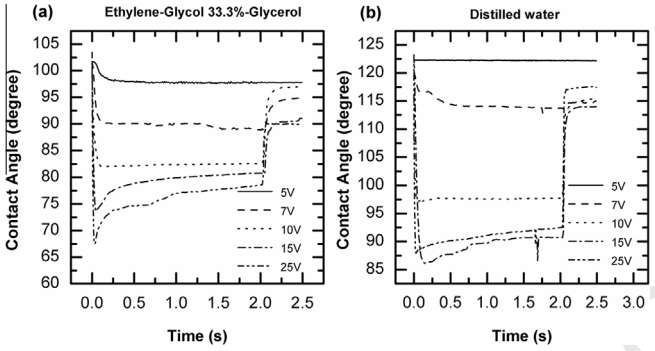

Highlights

• We have added a HDMS mixture to enhance contact angle variation and avoid cracks in the hydrophobic layer. • Low voltage actuation: contact angle changes from 7 V, achieving a change of 28° at 15 V for distilled water. • Comparison of distilled water and ethylene glycol glycerol mixtures analyzing contact angle change, recovery, falling time. • We have analyzed the actuation dynamics, achieving recoveries of more than 92% in all the cases, thus demonstrating the good reliability of the device.

Microelectronic Engineering xxx (2015) xxx–xxx

Contents lists available at ScienceDirect

Microelectronic Engineering

journal homepage: www.elsevier.com/locate/mee

EWOD using nonaqueous liquids

Maziar Ahmadi, Sandra Bermejo*, Luis Castañer

Grupo de Micro y Nano Tecnologías (MNT), Departamento de Ingeniería Electrónica, Universitat Politècnica de Catalunya (UPC), C/Jordi Girona 1-3, 08034 Barcelona, Spain

ARTICLE INFO

Article history:
Received 4 March 2015
Accepted 13 April 2015
Available online xxxx

Keywords:
Electrowetting
Non-aqueous liquid
Alumina
Reversibility

ABSTRACT

Electrowetting on Dielectric (EWOD) has been studied for more than a decade and used for different applications but still there are few works on non-aqueous liquids such as mixtures of polyols. We have found that significant contact angle change can be achieved at voltages of 10 V and bellow and that the recovery, when the voltage is withdrawn, exceeds 92% in all the cases. The dynamic change of contact angle has been measured applying 2 Hz and 5 Hz square 10 V amplitude signal. The operation is stable but has a cut-off frequency in the range of frequency explored. Those results have been achieved using a glass substrate covered by an ITO electrode followed by a thin alumina layer and by a Teflon layer. We have also observed that the use of an HMDS layer followed by an ALD alumina layer prior to Teflon deposition provides better initial contact angle value, and that it can be achieved a significant contact angle change at lower voltages. Up to 1000 switch cycles have been performed and the contact angle change when using DI water rapidly becomes insignificant whereas with the polyol mixtures, although we have observed contact angle change degradation, it gets to a stable value thereafter.

1. Introduction

The movement of liquids through channels based on Electrowetting on Dielectric phenomena (EWOD) [1–3], is being used in a large variety of Micro-Opto-Electro-Mechanical Systems (MOEMS) [4], such as liquid lenses [5], displays based on Electrowetting [6] or in a variety of biomedical sensors where liquid droplets are moved, merged and split [7–8]. In all those applications a thin electrode layer, a dielectric and a hydrophobic layer on top of each other, cover a substrate. When the liquid is electrically conductive, the drop movement is originated when an electric voltage is applied between a needle, or other kind of upper electrode, in contact with the drop, and a bottom electrode. As a result, the energy stored in the capacitor formed between the liquid and electrode unbalances the surface tension equilibrium leading to movement of the triple line [9–11]. This is schematically shown in Fig. 1. The main parameters are also shown.

In Fig. 1. γ_{SV} is the surface tension between the surface and air, γ_{LV} is the surface tension between the liquid and air, γ_{SL0} is the surface tension between the liquid and the substrate at zero voltage, θ is the macroscopic contact angle between the drop and the substrate and V is the applied voltage.

Distilled water is commonly used as liquid, either for simplicity or because it has a high surface tension value and high contact angle on hydrophobic surfaces. However, several problems have been observed such as corrosion of electrodes, electrolysis, bubbling, tendency to permeate through or swell numerous polymers, and ability to degrade some materials. Besides, water has a freezing temperature preventing its use in some outdoor electrowetting applications. As predicted by the Young–Lippmann equation [12], the contact angle gets smaller when the applied voltage increases until a certain saturation value is reached. Moreover, if the voltage value is reversed to zero, the contact angle does not fully recover the initial value [13].

All those problems have motivated the systematic research on non-aqueous liquids suitable for electrowetting applications [14] such as DMSO, ethylene glycol, formamide, γ-butyrolactone, N-methyl formamide, etc. and also, more recently, on room-temperature ionic liquids (RTILs) as electrolytes [15,16].

It is clear that achieving robust electrowetting devices requires further investigation in the main EWOD device elements: the hydrophobic layer and the liquid itself.

Among the non-aqueous liquids proposed in the literature, in this paper we have concentrated on mixtures of two organic liquids: ethylene glycol, which was studied by Heikenfeld [14] and a liquid which is widely used in microfluidics and in printed electronic applications: glycerol. However: ethylene glycol has low surface tension value and glycerol has a high viscosity value. A mixture of those components allows obtaining a workable electrowetting solution where surface tension is not too low and viscosity not too high to withstand the required speed of consumer

* Corresponding author. Tel.: +34 934054193
E-mail address: sandra.bermejo@upc.edu (S. Bermejo).

http://dx.doi.org/10.1016/j.mee.2015.04.085
0167-9317/

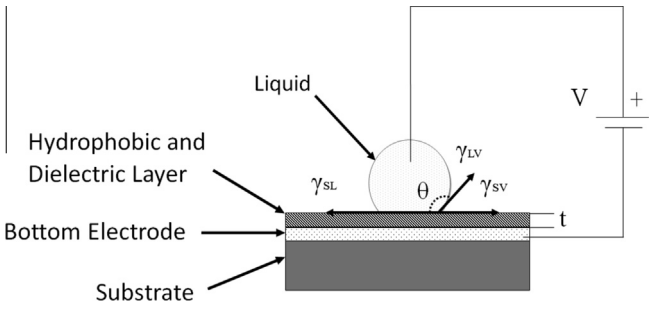

Fig. 1. Electrowetting on dielectric schematic side view.

applications. Moreover, mixtures of these liquids are commonly used as anti-freezing in automobiles and other outdoor applications depending on the mixture ratio [17]. In this work we have used different polar liquid mixtures (PLM) of ethylene–glycol and glycerol.

Moreover, we also have studied the dielectric layer and hydrophobic layer. As predicted by the Lippmann–Young equation, in order to reduce the value of the voltage required for a given change in contact angle, $\Delta\theta$, materials of larger value of the relative permittivity have to be used. Simultaneously, some treatment is required to avoid hydrolization and chemical reactions at the electrode. Among the many possibilities, Alumina (Al_2O_3) is a good candidate as, when deposited by atomic layer deposition (ALD) technique, it results in a very conformal layer, which is the origin of the reproducibility of the results. It also has a high relative permittivity value ($\varepsilon_r \approx 8$). These two properties allow to reduce the thickness of the Teflon layer and, hence, a lower actuation voltage is required for the same contact angle change [18]. For example, $\Delta\theta = 30°$ can be achieved at 25 V with a 25 nm thick alumina layer and a 150 nm Teflon layer on top.

We also have explored the effect of HMDS [19] as adhesion promoter prior to Teflon deposition process. HMDS (hexamethyldisilazane) is widely used in microelectronics industry to improve photoresist adhesion to oxides by a silylation process. HMDS works on surface oxides such as SiO_2, Al_2O_3, etc [20]. The compatibility with the semiconductor manufacturing process is the main reason to use this treatment in our samples with good results in enhancing hydrophobicity of Teflon layer as is shown below.

In this paper we have measured the initial contact angle, the dynamic change of the contact angle value after a given voltage is applied, the time response, the contact angle reversibility after the voltage is removed and the response of the liquid drop to a series of pulses of different frequencies. This study has been extended to 1000 pulse cycle in order to observe liquid behavior within EWOD phenomena for long term cycling.

2. Materials and experimental setup

The fabrication of our samples started by a sputtering deposition of a 76.7 nm thick indium–tin oxide (ITO) layer on a glass substrate as the bottom electrode. After the ITO electrode was deposited, a high relative permittivity dielectric material (high-k), namely, alumina (Al_2O_3), 25 nm thick layer was deposited by an atomic layer deposition (ALD) [21]. Before depositing Teflon layer [22], we deposited the adhesion promoter thin layer (HMDS) by spin-coating at 3000 rpm and then we typically completed the surface treatment by spin-coating, at 3000 rpm for 60 s, of a 10% Teflon AF solution (DuPont), resulting in a 200 nm thick film.

The film thickness was adjusted by varying the concentration of Teflon by diluting with Fluorinert FC-40 (DuPont). The Teflon-covered glass substrates were then heat treated for 6 min at 112 °C in air, followed by 5 min at 165 °C and 15 min at 328 °C, in order to remove any residual solvent and improve the adhesion of the Teflon layer to the substrate.

The liquids we have used in our experiments, are five different homogeneous mixtures of ethylene glycol and glycerol using 10 mL solvent (ethylene glycol) and several amounts of glycerol, resulting in glycerol percentage of 42.86%, 36.84%, 33.33%, 29.25%, 25%, 20%, 11.11%.

As the viscosity has very different values in ethylene glycol (1.61e−2 Pa s) and glycerol (1.412 Pa s), mixtures of the two liquids have a wide range of viscosity depending on the mixture percentage. The friction coefficient is linearly related to bulk viscosity and thereby affects the friction force at the triple line [23]. Experiments performed for several droplet volume and liquid viscosity show [24] that to remain in time response values of 10–20 ms viscosity should be smaller than 20–40 mPa s. As applications in this range of time response are the most probable (e.g. Lenses or displays) we have concentrated in the lower side of glycerol percentages in the mixtures.

The samples were placed onto a specific lens holder and goniometric device (CAM200) [25] to measure the contact angle, see Fig. 2, 10 μl drops of the conductive liquids were deposited using a vertical syringe on top of the surface of the samples. Side-view images of the drops were obtained using a high speed digital camera with zoom lens. A voltage difference was applied across the bottom electrode and a platinum needle in contact with the liquid with a power supply (Agilent 4156C) [26]. Typically, a 25 V negative voltage was applied to the platinum needle while the bottom electrode was grounded.

An automated, homemade surface and interfacial tension analyzer with high speed camera (BASLER A602F) [27] as front view, with resolution of 640 × 480 pixels with capturing speed rate of 400 f/s, and 640 × 480 pixels, 60 f/s camera as top view, was used. Real time image processing commercial software has been used to analyze the drop shape. Performing edge detection to extract the drop profile close to the contact line, the contact angle, θ, is obtained by evaluating the slope of a third order polynomial fit.

3. Results

In our experiments we observed that the layers of Teflon directly deposited on top of the ITO electrode suffered from breakdown after applying voltage between a droplet and the substrate. The results are shown in Fig. 3. where magnified pictures of the surface of Teflon before and after applying a 10 V to a DI water droplet are shown.

As can be seen, the application of voltage has produced a surface degradation jeopardizing the reproducibility of the measurements. This was totally avoided by depositing the alumina layer as described above, thereby demonstrating that alumina acts as a barrier avoiding Teflon damage.

The effect of the adhesion promoter HMDS treatment before Teflon deposition is shown in Fig. 4 where the values of the initial contact angle are shown for distilled water and for one of the mixtures of ethylene glycol and glycerol at 33%. In Fig. 4 an ITO plus alumina covered substrate with HDMS spun-on is compared with a similar substrate with Teflon 10% and with a third substrate with HDMS followed by Teflon 10%.

As can be seen, HMDS improves significantly the initial contact angle value in the two liquids.

In view of these results, we established as our baseline substrate the one having ITO, Alumina, HDMS treatment and Teflon 10% for the rest of the experiments.

We then analyzed different PLM of ethylene glycol–glycerol as alternatives to distilled water for many applications requiring high static contact angle and good and stable dynamic transient. In

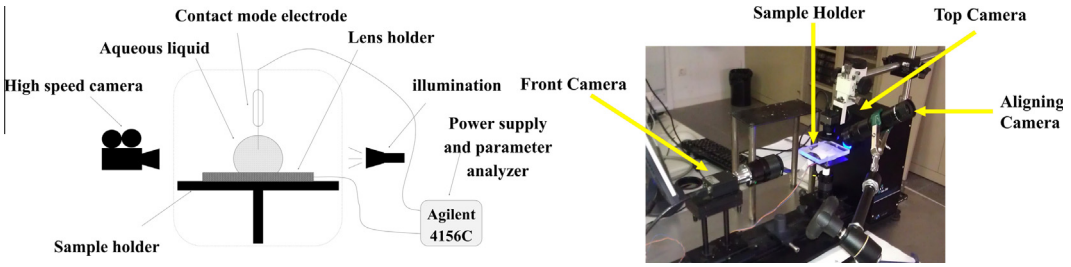

Fig. 2. Schematic of contact mode measurement setup (left) and picture of the experimental set-up (right).

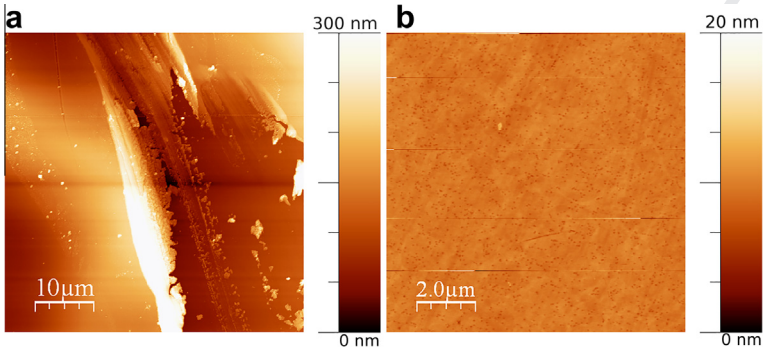

Fig. 3. (a) AFM image of Teflon 10% layer after applying 10 V, (b) AFM image of Teflon 10% layer before applying 10 V.

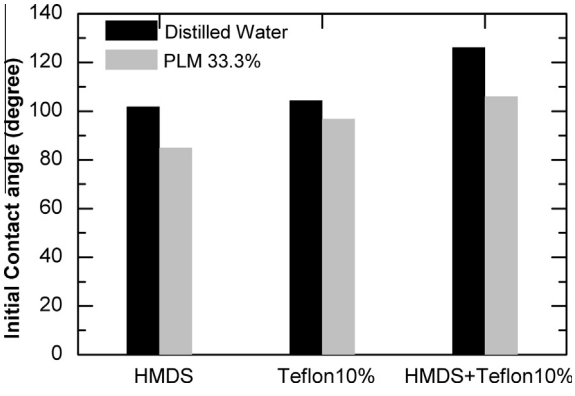

Fig. 4. Initial contact angle of distilled water and ethylene glycol–glycerol 33% mixture on different hydrophobic layers (only HMDS, only Teflon 10% and HMDS + Teflon 10%).

Fig. 5, lateral view of the drops showing the initial contact angle values are shown for our baseline substrate and for the various mixtures of liquids and distilled water for comparison. The values typically range between 101.7° and 106° slightly increasing with the glycerol concentration. The contact angle of distilled water was between 115° and 123°. These results show that the hydrophobicity of the surface has been enhanced by comparison with the 104° for distilled water on Teflon according to the datasheet. Moreover, a contact angle of 105.998° has been achieved for the largest glycerol concentration used in our experiments (PLM 33%).

Table 1 shows a comparison of the main parameters we have measured for an electrowetting experiment applying a voltage of 15 V in all cases to 10 μl droplets. As can be seen, the initial contact angle increases as the glycerol contents is increased and similar behavior is observed for the contact angle change $\Delta\theta$ and for the percentage of the contact angle recovery after the voltage is switched OFF. The contact angle change is significant even for this moderate value of voltage. We estimated also the fall time defined as the times between the 10% and 90% of the total angle change. Our measurements were performed using a time step of 0.01 s and in the lower contents of glycerol the fall time was smaller than the time resolution of the equipment. We also report on Table 1 the viscosity of the different mixtures of liquids. Fig. 6 shows the definitions we have used of the delay time t_d, the time to respond, t_r, and the difference between t_d and t_r that receives the name of fall time [28].

Fig. 7 summarizes the information provided in Table 1. In this polar plot the five main parameters studied in this work, are plotted for several mixture values of the polyol. We have shadowed the case corresponding to 33.3% mixture as our preferred choice for

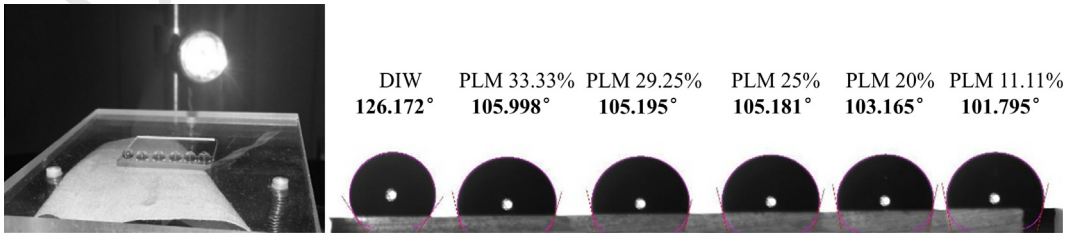

Fig. 5. Side pictures of liquid droplets of DIW and polar liquid mixtures (PLM).

Table 1
Conductivity and electrowetting measurements for several mixtures of ethylene glycol and glycerol for 15 V of applied voltage.

Liquid material	Viscosity (cP)	Initial contact angle (°)	Contact angle change (°)	Fall time (s)	Contact angle recovery (%)
PLM 11.11%	37.3	101.7945	15.131	0.01	92
PLM 20%	60.2	103.1655	9.65	0.08	93
PLM 25%	65.4	105.181	12.841	0.095	95
PLM 29.25%	73.7	105.1955	12.2105	0.08	95
PLM 33.33%	92.8	105.9975	20.4195	0.06	97
PLM 36.84%	94.2	103.808	7.033	0.048	95
PLM 42.86%	120.6	96.879	6.869	0.06	91

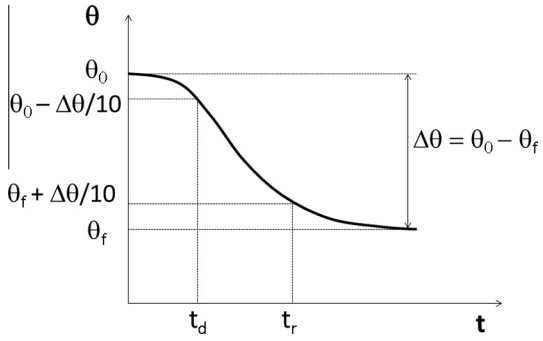

Fig. 6. Definitions of the delay time t_d, the time to respond, t_r, and the difference between t_d and t_r that receives the name of fall time.

more detailed analysis as this mixture exhibits a good trade-off among maximum recovery, contact angle variation and short delay and falling time.

In Table 2 we summarize our results on the contact angle change, fall time and contact angle recovery percentage for distilled water and the 33% mixture of ethylene–glycol and glycerol for several values of the applied voltage. As can be observed, significant change of contact angle can be achieved at voltages less than 25 V. The fall time decreases as the voltage is increased, although this has to be taken cautiously, as in the larger voltages the transient has an overshoot and then the relevant figure should

Table 2
Summary of electrowetting measurements for distilled water and 33% mixture of ethylene glycol and glycerol for several values of applied voltage.

Liquid droplet	Voltage (V)	Contact angle change (°)	Fall time (s)	Contact angle recovery (%)
Distilled water	5	0.24	–	–
	7	6.35	0.17	95.74
	10	18.63	0.11	100
	15	36.99	0.15	92.57
	25	35.33	0.04	95.32
	50	37.23	0.03	87.71
Ethylene glycol–glycerol 33%	5	3.83	0.43	96.12
	7	11.66	0.33	93.40
	10	19.48	0.12	95.71
	15	27.21	0.03	95.51
	25	35.95	0.03	86.97
	50	37.78	0.01	86.82

be the settling time (time required to reach the steady state value) instead of the fall time. These results in Table 2 show that the Alumina-Teflon stack layer allows for low voltage operation, good recovery and fall time in the range of tens of milliseconds for 15 V. Taking into account the different values of the initial contact angle, Table 2 also shows the percentage recovery, as can be seen a recovery greater than 85% is observed in all cases and the ethylene glycol–glycerol mixtures recover quite similarly to water. Fig. 6 shows the definition of delay time, response time and falling time.

We have also performed full transient measurement of the contact angle using the ethylene glycol–glycerol 33% mixture for several voltages, namely 5, 7, 10, 15 and 25 V and compare it with distilled water. This is shown in Fig. 8 where the transients registered for a 10 μl droplet. The transients shown are a sequence of an OFF_ON switch followed by an ON_OFF switch after 2 s. We can observe that the transients exhibit a sharp drop of the contact angle value when the voltage is applied and, in the case of larger voltages, an overshoot is observed followed by a stabilization phase toward a steady state value. In all cases we can interpret the results as over-damped transients.

In Fig. 9 shows a plot of the $(\cos\theta - \cos\theta_0)$ value, where θ is the contact angle at the steady state (taken at a time $t = 2$ s just before

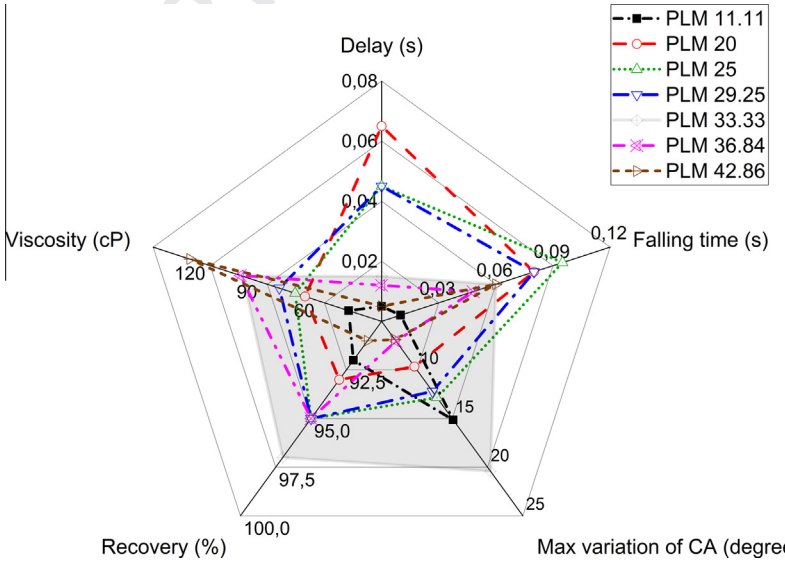

Fig. 7. Polar plot of the five main parameters studied in this work, plotted for several mixture values of the polyol. We have shadowed the case corresponding to 33.3% mixture as our preferred choice.

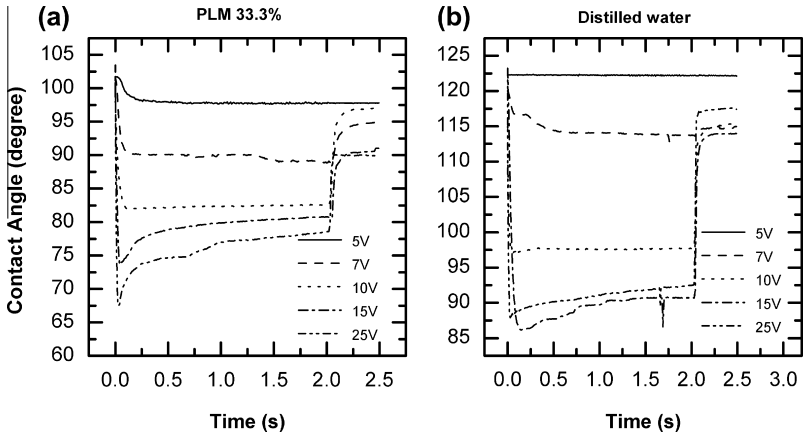

Fig. 8. Transient contact angle by applying a step voltage of OFF–ON–OFF for 2 s with 5, 7, 10, 15, 25 V to distilled water 10 μl and PLM 33%.

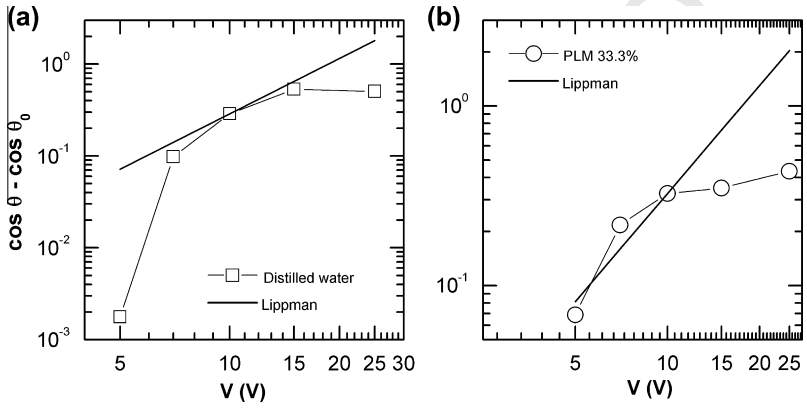

Fig. 9. Plot of the value of the difference $(\cos\theta - \cos\theta_0)$ as a function of the applied voltage for: (a) distilled water, and (b) PLM 33.3%.

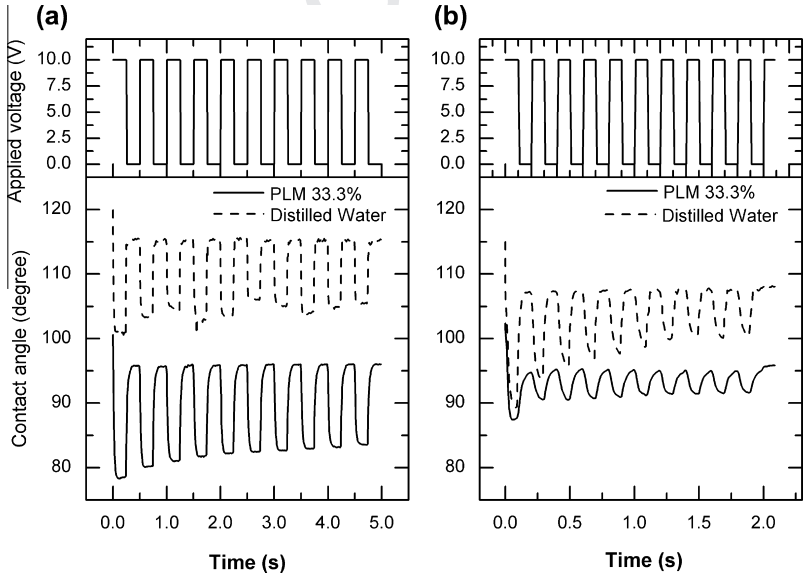

Fig. 10. Dynamic EWOD measurements on distilled water and ethylene glycol–glycerol 33% for: (a) 2 Hz and (b) 5 Hz 10 V amplitude signal.

the voltage is removed), and θ_0 is the initial contact angle value. The values of are plotted as a function of the applied voltage V. The logarithm of the Lippmann–Young equation can be written as,

$$\log\ (\cos\theta - \cos\theta_0) = \log\frac{\varepsilon_r\varepsilon_0}{2h\gamma} + 2\log\ V \qquad (1)$$

where h is the thickness of the dielectric, γ is the surface tension ε_0 is the vacuum permittivity ε_r is the relative permittivity of the dielectric layer and V is the applied voltage between the droplet and the substrate. It is clear from Eq. (1) that the value of the slope of the plot of $\log(\cos\theta - \cos\theta_0)$ as a function of $\log V$ should have a value of 2. Our best fit of the Lippmann–Young equation in Fig. 9 in

the range where it holds in the experiments, gives us a value of the electrowetting factor ($\varepsilon_0\varepsilon_r/2h\gamma$) of 3.25e−3 for the ethylene glycol–glycerol mixture and 5.23e−3 for water. We also see that the contact angle saturation is reached for voltages between 10 and 15 V in all cases.

EWOD devices are to become the mainstream technology for a number of applications such as lab on chip or liquid lenses and this is why the commutation properties of the liquid have to withstand many switching cycles. In order to see how the experiments performed in this work behave under a square signal of given amplitude and frequency, we have registered the dynamic contact angle when a 10 V amplitude, 2 Hz (Fig. 10a) and 5 Hz (Fig. 10b) frequency were applied. The results are shown in Fig. 10.

We can observe that the 33.3% mixture of ethylene glycol–glycerol reaches a regime of almost constant amplitude after the first few cycles have elapsed. On the contrary, the distilled water behavior is more uncertain concerning the contact angle change. If we increase the signal frequency to 5 Hz, the result is shown in Fig. 10b. There we can see that we are over the frequency band-pass of the system and stable values after every switch are not reached, although the 33.3% mixture of ethylene glycol–glycerol has a periodic shape. This would mean that the cut-off frequency of the system explored in this work is in the range of 2–5 Hz for 10 μl droplets.

In order to analyze potential degradation of the contact angle change from the ON to OFF voltage, we have registered up to 1000 cycles of 10 V amplitude signal to both distilled water and PLM 33.3% samples (Fig. 11). Fig. 11a shows a very fast degradation of the contact angle change in the first 100 cycles approximately and after that, the droplets of the distilled water are practically insensitive to the applied voltage change. This is more clearly illustrated in Fig. 11b, where the difference in contact angle as a function of time is plotted. On the contrary the droplets of PLM mixture at 33.3% (Fig. 11d), although a degradation is also observed, it gets, in approximately the first 30 cycles, to a steady state regime with an stable contact angle change of 10°.

Fig. 12 shows an staircase up and down voltage ramp to further explore the dynamic recovery of the DIW and of the PLM. Results show that, looking at the recovery part of the picture, DIW droplet seems to lag behind the voltage stair case and a kind of memory effect is observed. On the contrary, the droplet of PLM 33.33% fully recovers without significant delay.

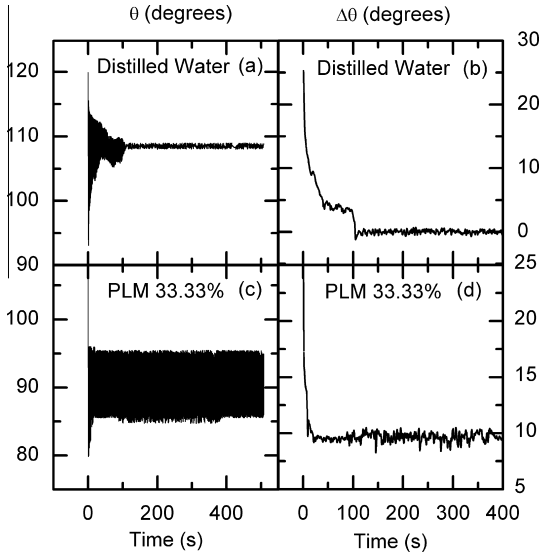

Fig. 11. Applying 1000 cycles of 10 V amplitude signal to both distilled water and PLM 33.3% samples.

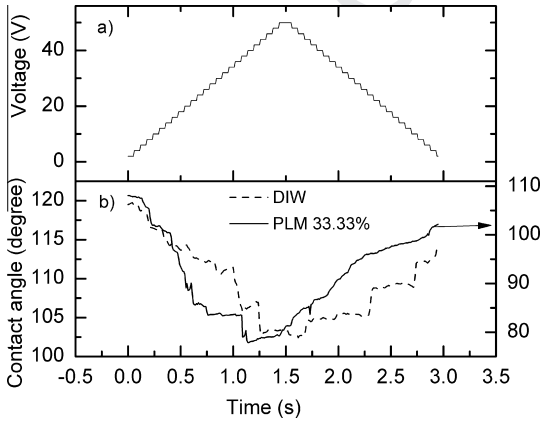

Fig. 12. (a) Staircase up and down voltage ramp and (b) dynamic recovery of the DIW and of the PLM.

4. Conclusions

In this work we report several electrowetting experiments using non aqueous liquids and compare with distilled water. We have found that the integrity of the Teflon layer is better preserved if an alumina barrier layer is deposited prior to the Teflon and HDMS is used as adhesion promoter. Additionally, low voltage electrowetting is achieved as the layer of Alumina also allows the use of a thinner layer of Teflon while avoiding breakdown or damage of Teflon layer. We have improved the hydrophobicity of Teflon layer just by spin-coating HMDS prior to Teflon layer deposition. We have analyzed different mixtures of ethylene glycol with glycerol and have compared them to distilled water, demonstrating that these non-aqueous liquids can be an alternative to water in terms of contact angle change, time response and recovery.

Acknowledgements

This work has been partially supported by the Spanish Ministry of Science and Innovation under project TEC2010-18222. The authors would like to thank Gema López for her fruitful help.

References

[1] W.C. Nelson, C.-J. Kim, J. Adhes. Sci. Technol. ahead-of-p (2012) 1–25, http://dx.doi.org/10.1163/156856111X599562.
[2] S.K. Cho, H. Moon, C.-J. Kim, J. Microelectromech. Syst. 12 (2003) 70–80, http://dx.doi.org/10.1109/JMEMS.2002.807467.
[3] J. Lee, H. Moon, J. Fowler, T. Schoellhammer, C.-J. Kim, Sens. Actuators A Phys. 95 (2002) 259–268, http://dx.doi.org/10.1016/S0924-4247(01)00734-8.
[4] F. Gindele, F. Gaul, T. Kolling, Photon. Eur. (2004).
[5] Varioptic – Liquid Lens Solutions, Auto Focus M12 and C-mount Lens Modules, n.d. <http://www.varioptic.com/> (accessed 24.07.14).
[6] Home – Liquavista – Electrowetting Based Low Power, Always Viewable Color Video Displays, n.d. <http://www.liquavista.com/> (accessed 24.07.14).
[7] S. Chen, P.Y. Keng, R.M. Van Dam, C. Kim, Synthesis of 18 f-labeled probes on EWOD platform for positron emission tomography (pet) preclinical imaging, Crump Institute for Molecular Imaging, 4 Mechanical and Aerospace Engineering Dept., 2011. 980–983.
[8] S. Chen, A.A. Dooraghi, M. Lazari, R.M. van Dam, A.F. Chatziioannou, C.-J.C. Kim, 2014 IEEE 27th Int. Conf. Micro Electro Mech. Syst., 2014, pp. 284–287, http://dx.doi.org/10.1109/MEMSYS.2014.6765631.
[9] L. Castañer, V. Di Virgilio, S. Bermejo, Langmuir 26 (2010) 16178–16185, http://dx.doi.org/10.1021/la102777m.
[10] I. Drygiannakis, G. Papathanasiou, G. Boudouvis, J. Colloid Interface Sci. 326 (2008) 451–459, http://dx.doi.org/10.1016/j.jcis.2008.06.061.
[11] J.-L. Lin, G.-B. Lee, Y.-H. Chang, K.-Y. Lien, Langmuir 22 (2006) 484–489, http://dx.doi.org/10.1021/la052011h.
[12] G. Lippmann, Ann. Chim. El Phys. 5 (1875) 494–549.
[13] J. Restolho, J.L. Mata, B. Saramago, J. Phys. Chem. C 113 (2009) 9321–9327, http://dx.doi.org/10.1021/jp902393r.

[14] S. Chevalliot, J. Heikenfeld, S. Member, L. Clapp, A. Milarcik, J. Display Technol. 7 (2011) 649–656.
[15] S. Millefiorini, A.H. Tkaczyk, R. Sedev, J. Efthimiadis, J. Ralston, J. Am. Chem. Soc. 128 (2006) 3098–3101, http://dx.doi.org/10.1021/ja057606d.
[16] J. Restolho, J.L. Mata, B. Saramago, J. Colloid Interface Sci. 340 (2009) 82–86, http://dx.doi.org/10.1016/j.jcis.2009.08.013.
[17] A.W. Adamson, A.P. Gast, Physical Chemistry of Surfaces, 6th ed., n.d.
[18] S. Berry, J. Kedzierski, B. Abedian, J. Colloid Interface Sci. 303 (2006) 517–524, http://dx.doi.org/10.1016/j.jcis.2006.08.004.
[19] D. Chatterjee, H. Shepherd, R.L. Garrell, Lab Chip. 9 (2009) 1219–1229, http://dx.doi.org/10.1039/b901375j.
[20] M. Madou, Fundamentals of Microfabrication: the Science of Miniaturization, 2nd ed., CRC Press, 2000. p. 10.
[21] S.M. George, Chem. Rev. 110 (2010) 111–131, http://dx.doi.org/10.1021/cr900056b (accessed 24.07.14).
[22] H. Tavana, N. Petong, A. Hennig, K. Grundke, A.W. Neumann, J. Adhes. 81 (2005) 29–39, http://dx.doi.org/10.1080/00218460590904435.
[23] H. Li, M. Paneru, R. Sedev, J. Ralston, Langmuir 29 (2013) 2631–2639.
[24] J. Hong, Y.K. Kim, K.H. Kang, J.M. Oh, I.S. Kang, Langmuir 29 (2013) 9118–9125.
[25] CAM200 (KSV NIMA), n.d. <https://cit.kuleuven.be/smart/infrastructure/documents/cam200.pdf> (accessed 24.07.14).
[26] 4156C Precision Semiconductor Parameter Analyzer [Discontinued]|Agilent, n.d. <http://www.home.agilent.com/en/pd-153517-pn-4156C/precision-semiconductor-parameter-analyzer?&cc=ES&lc=eng> (accessed 24.07.14).
[27] Basler Industrial Cameras – A600 Series – A602f, n.d. <http://www.baslerweb.com/products/A600.html?model=313> (accessed 24.07.14).
[28] L.W. Turner, Electronics Engineer's Reference Book, 4th ed., Butterworth & Co, 1976.